
Improving the Estimation of the COVID-19 Effective Reproduction Number using Nowcasting

Joaquín Salas¹

Journal Title
XX(X):2–18
©The Author(s) 2016
Reprints and permission:
sagepub.co.uk/journalsPermissions.nav
DOI: 10.1177/ToBeAssigned
www.sagepub.com/

SAGE

Abstract

As the interactions between people increases, the impending menace of COVID-19 outbreaks materialize, and there is an inclination to apply lockdowns. In this context, it is essential to have easy-to-use indicators for people to use as a reference. The effective reproduction number of confirmed positives, R_t , fulfill such a role. This document proposes a data-driven approach to nowcast R_t based on previous observations' statistical behavior. As more information arrives, the method naturally becomes more precise about the final count of confirmed positives. Our method's strength is that it is based on the self-reported onset of symptoms, in contrast to other methods that use the daily report's count to infer this quantity. We show that our approach may be the foundation for determining useful epidemic tracking indicators.

Keywords

Effective Reproduction Number, Basic Reproduction Number, Compounded Rate of Change, COVID-19

Introduction

After a period of confinement due to the presence of COVID-19 and facing economic and social pressures, societies start to open up, seeking to return to productive, sport, and recreational activities. As the interactions between people increase, the impending menace of outbreaks materializes. Naturally, there is a tendency to apply once again lockdowns, in what has been called *the hammer and the dance*¹. In this context, it is essential to have easy to apply indicators for people to use as a reference. At the beginning of the infection, when all population members are susceptible, the average number of illnesses that an infected person originates is called the basic reproduction number, R_0 . Sometime after the beginning of the infection, and with considerably more practical utility, one may want to know the effective reproduction number, R_t ². When R_t is higher than one, the number of infected people grows exponentially, *i.e.*, their number will double in a short period. When R_t is less than one, the epidemic will tend to disappear. However, estimating R_t accurately at the required level of geospatial resolution is a complex problem.

Although applicable to any country, let us take the case of Mexico as an example. The records generated by the epidemiological surveillance system contain information that includes, among other predictors, the number of confirmed positives, deaths, and suspects. Daily, the Ministry of Health informs the public about the status of its records³. However, the data it discloses updates records of events that occurred in the past, sometimes as far as 90 days ago. At other times, with a significant frequency, the records that were previously released are discarded. Although publishers often drop these erroneous entries overnight, there have been cases of records eliminated after more than 50 days.

Besides the integrity of the information, there are other difficulties in tracking the epidemic inherent to the pandemic and interesting for researchers, decision-makers, and the general public. SARS-CoV-2 is an airborne virus⁴, which infects some people without causing symptoms⁵.

¹ CICATA Querétaro, Instituto Politécnico Nacional

Corresponding author:

Joaquin Salas, Instituto Politécnico Nacional, Cerro Blanco 141, Colinas del Cimatarío, Querétaro, México
Email: salas@ieee.org

On a significant number of occasions, people begin to spread COVID-19 before they start to feel sick⁶. Also, each infected person reacts differently and will have, if anything, a different latency and incubation period⁷. People will have a different contagious period, manifested with unequal intensity during that time⁸. Although the symptoms are known, one may reveal them differently. People will require different types of medical attention, which may or may not require hospitalization⁹. In some cases, someone ill may need or not a ventilator¹⁰. Eventually, a given person may recover, possibly with sequels, or will pass away¹¹. About the whole process, we begin to have some statistical knowledge on which we can develop models. In this paper, propose a data-driven approach that leverage experience to create a simple, yet effective nowcasting method for R_t that can be used by policy-makers as well by the general public. Our main contribution is an approach to use past observations to generate plausible sequences of estimates for the number of confirmed positive cases that could have possibly occurred in the recent days to compute variations of the effective reproduction number.

We base our method on the statistical behavior of previous observations. As more information arrives, the estimation naturally becomes more precise about the final count of confirmed positives. In the next section, we review the literature about related methods. Then, we proceed to discuss the intrinsic delay in information flow that exists in the process of detecting a COVID-19 confirmed positive and detail our approach to estimate plausible sequences for the number of infected people. This insight leads us to review the underlying method we employ to calculate the effective reproduction number using the health reports available. After showing some results of our implementation of the nowcasting method for R_t , we conclude our study by discussing and delimiting our findings and delineating some potential research lines.

Related Literature

Though recent, COVID-19 has kickstarted some novel ideas to track it reliably. The research effort to nowcast the basic reproduction number can be classified in either mechanistic approaches, Bayesian approaches, or a hybrid combination of both.

Mechanistic Approaches

Wang *et al.*¹² developed a hybrid model to complement the dynamics of the SIR (Susceptible, Infectious, Recovered) model with spatiotemporal analysis. The space-time component is modeled, at the start, with a Poisson distribution to describe rare events. Then, they complemented it with a negative binomial random model during over-dispersion. Balabdaoui and Mohr¹³ propose an age-stratified discrete compartment model as an alternative to SIR type models. Their approach follows the trajectory of individuals that includes the exposed, the asymptomatic, the symptomatic infectious, the symptomatic in self-isolation, the patients in the intermediate care unit, and the patients in the intensive care unit. Masjedi *et al.*¹⁴ compares phenomenologic and mechanistic models. The former based on generalized Richards models¹⁵ (an extension of sigmoid functions) and the latter on a modified SEIR (Susceptible, Exposed, Infectious, and Recovered) model. They fit the models with observed data to forecast the next month. They observe that although phenomenologic models fit the data, they are not reliable for decision-making. In contrast, SEIR models predicted the phenomena better. Contaldi¹⁶ presents SIRFH, an extension of the SIR model that tracks hospitalizations and hospital-based fatalities introducing additional differential equations. The estimation for the basic reproduction number derives from the solution to this extended model. Finally, Annan and Hargreaves¹⁷ produce a nowcasting method based on the SEIR model. To calibrate the parameters, they use observational data and a Bayesian approach. Annan and Hargreaves' analysis includes the uncertainties associated with deaths' stochastic nature, the reporting errors, and the model itself.

Bayesian Approaches

Altmejd *et al.*¹⁸ present a model based on the removal method¹⁹, where one extracts batches of a fixed population. Their models deal with lags arising from the calendar patterns, where events reported during the weekends are less. Their Bayesian approach uses a likelihood that considers the number of reports by day of the week, and priors with improper uniform distribution. Their model provides better estimates than seven days averages. Schneble *et al.*²⁰ present a nowcasting model based on the number of deaths, as quantifying their correct number is more reliable than for infected people. Their epidemic spread model considers

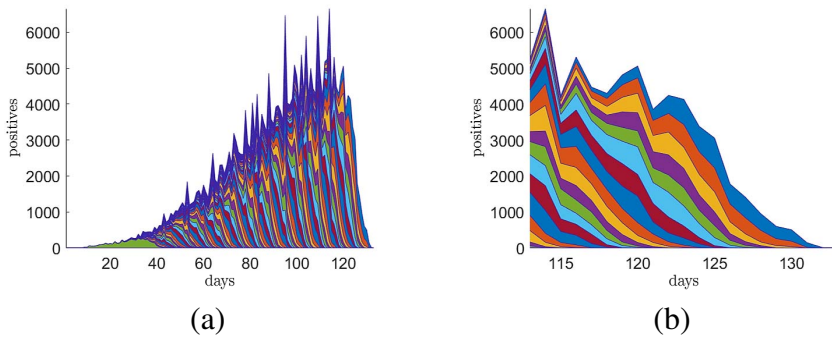


Figure 1. Delays in reporting. The horizontal axes show the day of onset. The vertical axes indicate the number of patients confirmed positives. In (b), we zoom in on the last 30 days shown in (a). Each layer is an update to registers in the past.

region and age-specific Poisson distributions, where they consider lag to report. They model the effect of age, gender, weekday, and location as a quasi Poisson distribution. Then, they infer a posterior using a Gaussian prior. For nowcasting, they model the delay as a random variable which will provide death counts. They distribute these death counts as a quasi-binomial distribution. Chitwood *et al.*²¹ propose to use a Bayesian framework for nowcasting. They take into account delayed and incomplete reporting. They assume that one can understand the COVID-19 complex spread system by examining the individual components. In that model, they consider the uncertainty that results from available diagnosis and delays in the estimation of disease progression and reporting systems. Lastly, Abbot *et al.*²² employ a quasipoisson regression model to estimate the spread rate. Interestingly, they base their analysis on the reported dates for the confirmed positives and infer the symptom onset through statistical modeling.

Characterizing the Update Pattern

In our approach, we characterize the frequency at which the counting updates of COVID-19 confirmed positives occur. In this section, we analyze the origin of such delays and describe the form we model them.

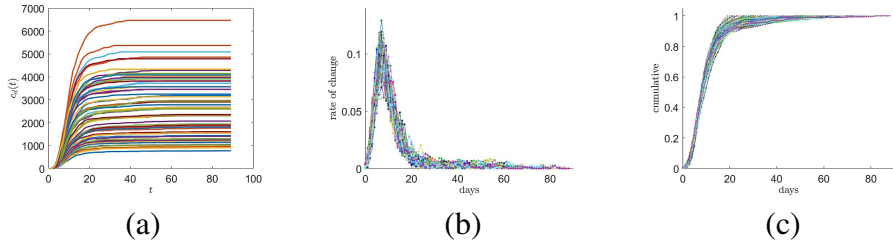


Figure 2. Confirmed positives. (a) As the days pass, updates eventually level off to a final count for a given day $C_t(D)$. (b) and (c) show the normalized daily number of reported confirmed positive and the accumulated number of cases. Our method relies on the assumption that it is possible to model the daily variations with a data distribution.

Delays in the Report of Confirmed Positives

Declaring a person confirmed positive involves a complex process that may take days, even nowadays, when it is of paramount importance to achieve certainty for decision-making. Just consider the case of a person showing symptoms related to COVID-19²³ that decides to visit the physician. After an interview to collect some necessary clinic information, the physician chooses to take either a sample from the nasopharynx using a long swab²⁴ or a CT (Computer Tomography)²⁵. In some places, the sample can be analyzed via the RT-PCR(reverse-transcription polymerase chain reaction)²⁶ *in situ* with results on the same day but frequently it may take a week or longer to be processed. Afterward, the results will be uploaded in computer systems and summarized for analysis.

In Figure 1, we illustrate the effect of delays in reporting using the data set made public by the Mexican Health Ministry³. The horizontal and vertical axes show the day of onset and the number of confirmed positive cases. Each layer corresponds to the number of cases added to a prior date. Although the number of updates may be significant for a given day, they eventually converge to the total number of confirmed positives for that day, $C_t(D)$, for D large, and where t expresses the day of interest (see Figure 2(a)). If we divide the daily accumulated of confirmed positives $C_t(\delta)$, for a given day δ , by $C_t(D)$, the cumulated distribution will tend to one. We illustrate this in Figure 2(b)-(c), where we show both, the rate of daily change and the cumulative change. Our approach aims to characterize the variations we observe in these distributions to develop a model for nowcasting.

Compounded Rate of Change

We aim to estimate the number of confirmed positive cases $C_t(D)$ for the day t using the following δ days of reports available. In principle, we would learn about $C_t(D)$ when D is considerably large. But in practice, D can be as short as one month and a half of daily updates. Given the number of confirmed positives δ days after day t , $C_t(\delta)$, the number of confirmed positives on day $C_t(\delta + 1)$ can be expressed as

$$C_t(\delta + 1) = C_t(\delta)(1 + \rho_t(\delta)), \quad (1)$$

where $\rho_t(\delta)$ is the rate of change from one day δ to the next $\delta + 1$, for reference day t . If we solve the recursion, we will have the expression

$$C_t(D) = C_t(0) \prod_{\delta=0}^{D-1} (1 + \rho_t(\delta)), \quad (2)$$

where one assumes that the daily rate changes over time. In the cases we are studying, the curves expressing the rate of change of the number of confirmed positive relative to the day before, for a different starting day, seem to be somewhat consistent over the samples. We model ρ_t as a random variable, which follows a probability distribution we may infer from the experimental samples. Then, on the day $t + \delta$, the best-guess prediction for the number of confirmed positive, $C_t(\delta)$, is

$$C_t(D) = C_t(\delta)(1 + \rho_t^D(\delta)), \quad (3)$$

where our newly defined random variable $\rho_t^D(\delta)$ expresses the rate of change from day $\delta + t$ to day D . In our approach, we model $\rho_t^D(\delta)$ as a random variable with different distribution for each day δ , for more fine-grained or longer-term prediction. One may find the relationship between $\rho_t^D(\delta)$ and $\rho_t(\delta)$ by noting that (2) and (3) solve for $C_t(D)$ as

$$C_t(0) \prod_{\delta=0}^{D-1} (1 + \rho_t(\delta)) = C_t(\delta)(1 + \rho_t^D(\delta)). \quad (4)$$

Expanding $C_t(\delta)$ using the recurrence relationship in (1), we have

$$C_t(0) \prod_{\delta=0}^{D-1} (1 + \rho_t(\delta)) = C_t(0) \prod_{d=0}^{\delta-1} (1 + \rho_t(d))(1 + \rho_t^D(\delta)), \quad (5)$$

from where, after eliminating for the common factors, solving for $\rho_t^D(\delta)$ results in

$$\rho_t^D(\delta) = \prod_{d=\delta}^{D-1} (1 + \rho_t(d)) - 1. \quad (6)$$

Effective Reproduction Number R_t

Given a particular sequence of the observed number of infected people $\{C_0(\delta), C_1(\delta - 1) \dots, C_t(0)\}$, and the argument of the number of days the report has been updated, we aim to nowcast the basic reproduction number R_t , *i.e.*, given the distribution of the rate of change $\rho_t^D(\delta)$, we generate ensembles of sequences aiming to estimate $\{C_0(D), C_1(D) \dots, C_t(D)\}$ before proceeding to calculate R_t . We first review *EpiEstim*, a method proposed by Cori *et al.*²⁷, to estimate R_t from the observed number of cases.

Cori *et al.*²⁷ proposed a Bayesian framework to compute R_t , where the number of infected people observed at day t , C_t , follows a Poisson process. In a simplification, they assume that the daily observations of infected people are independent. Thus, one may express the likelihood of observing a sequence of infected people between day $t - \tau - 1$ and day t as²⁷

$$P(C_{t-\tau+1}, \dots, C_t \mid C_0, \dots, C_{t-1}, \mathbf{w}, R_{t,\tau}) = \prod_{s=t-\tau+1}^t \frac{(R_{t,\tau}\Lambda_s)^{C_s} e^{-R_{t,\tau}\Lambda_s}}{C_s!}, \quad (7)$$

where the transmissibility $R_{t,\tau}$ is assumed to be constant over the period $[t - \tau + 1, t]$, $\Lambda_t = \sum_{s=1}^t C_{t-s} w_s$ is the total infectiousness of infected people at time t , and $\mathbf{w} = (w_1, \dots, w_t)^T$ is a mass density probability profile of infectivity profile for an individual. Cori *et al.*²⁷ assume that the effective reproduction number $R_{t,\tau}$ is a random variable which probability follows a Gamma distribution as²⁷

$$P(R_{t,\tau}) = \frac{R_{t,\tau}^{a-1}}{\Gamma(a)b^a} e^{-R_{t,\tau}/b}, \quad (8)$$

where a and b are the parameters of shape and scale. Since the Poisson and Gamma probability distributions are conjugate, one can express the

posterior in closed form, again as a Gamma distribution, as²⁷

$$P(C_{t-\tau+1}, \dots, C_t, R_{t,\tau} \mid C_0, \dots, C_{t-\tau}, \mathbf{w}) \propto R_{t,\tau}^{\alpha-1} e^{R_{t,\tau}/\beta} \prod_{s=t-\tau+1}^t \frac{\Lambda_s^{C_s}}{C_s!}, \tag{9}$$

from where the mean α and standard deviation β are given by

$$\alpha = a + \sum_{s=t-\tau+1}^t C_s \text{ and } \beta = \frac{1}{\sum_{s=t-\tau+1}^t \Lambda_s + \frac{1}{b}}. \tag{10}$$

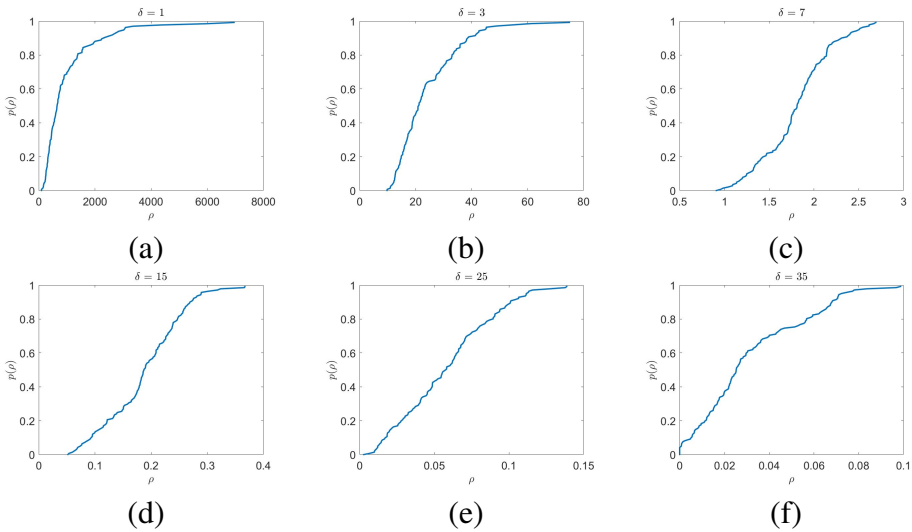
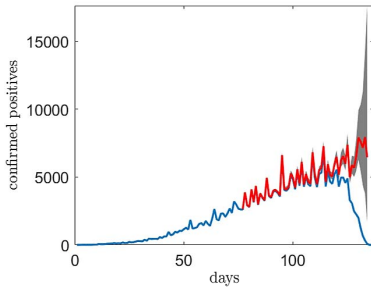
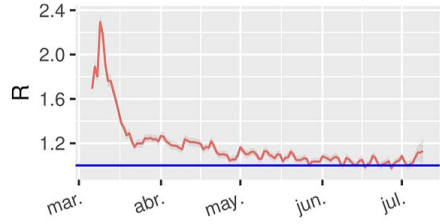
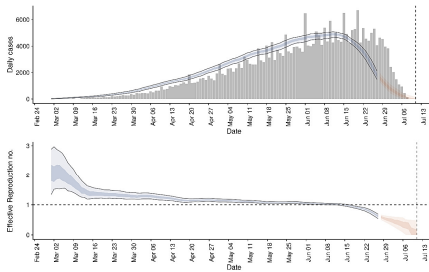


Figure 3. Empirical Distribution Function. Out of the historical observations, we construct distributions for ρ . Here, we show examples for $\delta = 1, 3, 7, 15, 25, 35$.

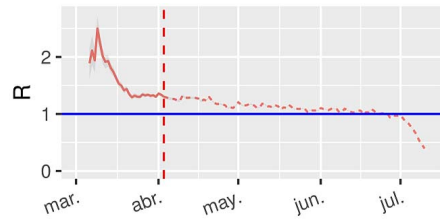
Given $C_t(\delta)$, the information about the number of infected people δ days after the day of interest t , and the model for the probability function for $\rho_t^D(\delta)$, we produce N random samples which will correspond to the number of people infected that day. We then compute R_t for each of the sequences using the model proposed by Cori *et al.*²⁷. Finally, we calculate the mean and standard deviation for R_t to provide the most likely value and uncertainty at one standard deviation. To take into account the



(a) Nowcasting the infected

(b) $R_t = 1.3 \pm 0.113$ 

(c)



(d) Without nowcasting

Figure 4. Qualitative comparison of the model's output. For the daily confirmed cases (a), we show Cori's output *et al.* algorithm to compute R_t . We fed the data to the method provided by Abbott *et al.*²², which seems to follow the reported daily cases. Finally, we illustrate the output of our approach, including its area of uncertainty.

difference between the accepted values for the average incubation (five days)⁷ and latency periods (three days)⁶, we represent them two days before t .

Results

We took the data set for COVID-19 cases provided by the Mexican Health Ministry corresponding to July 11, 2020. The data set contains 723,668 records, out of which 295,268 correspond to confirmed positives. As time passes by, the number of confirmed positives for a given day t is updated. In Figure 1, we illustrate how each day the updates stack up a layer of updated registers toward the past. As we accumulate the number of confirmed positive updates, we observe that the total quantity levels off and reaches a maximum at $C_t(D)$ (see Figure 2). About 98% of reports

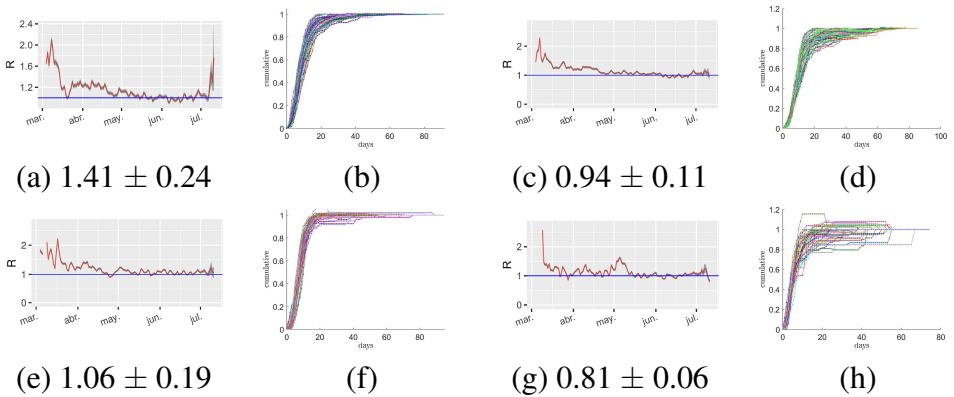


Figure 5. Estimation of R_t for some states of Mexico and corresponding cumulative normalized distribution for Mexico City (a)-(b), Mexico State (c)-(d), Tabasco (e)-(f), and Queretaro (g)-(h).

are filled out by day 33. When we divide the daily updates for the day t by $C_t(D)$, we obtain the normalized updates by day and accumulated registers illustrated in Figure 2.

We then proceed to construct empirical distributions describing the variation of $\rho_t^D(\delta)$. We show illustrations of this for $\delta = 1, 3, 7, 15, 25$ and 35 in Figure 3. Note that $\delta = 0$ is not present as generally the number of reported confirmed positive for $C_t(0) = 0$ causing $\rho_t(0)$ to be undefined. Once we have the models for $\rho_t(\delta)$, we may proceed to generate estimates for the number of confirmed positives for $C_t(D)$ using (3). The mean and standard deviation statistics will provide us with the most likely value and an estimate for the uncertainty. We use the same set of randomly generated values to obtain sequences, which we evaluate using the method proposed by Cori *et al.*²⁷ to obtain the instantaneous R_t . Our implementation considers the pre-symptomatic transmission, *i.e.*, the incubation period, or the time it takes for an infected person to start showing symptoms, is greater than the latent period, or the time from which an infected person can spread to others. Following Bar-On *et al.*²⁸, we assume that the latent period lasts for three days and the incubation period for five days.

We compare the performance of our nowcasting with the proposed by Abbott *et al.*²² (see Figure 4). In their case, the nowcasting tends to closely follow the number of reported confirmed positives, which gives the undesirable effect of resulting in a descending R_t , when it is not.

Our proposal, on the other hand, increases its certainty naturally as more information is available.

As we increase δ in our nowcasting exercise, there is a tendency to observe fewer cases, because there has not been enough time for the information to arrive. We set a dynamic threshold to stop the nowcasting estimation when for a particular day of analysis, δ , the number of confirmed positive cases is less than 30. Also, we have observed that as the number of confirmed positive is less, the normalized cumulative curves tend to be noisier. In Figure 5, we illustrate what happens for entities in Mexico where the number of confirmed positive cases is 59,667 (Mexico City), 44,114 (State of Mexico), 15,909 (Tabasco), and 2,667 (Querétaro). We believe that our method works best when the number of positive cases is beyond 2,600 for the observed interval of 90 days. Using this threshold, there are still currently 30 States (out of 32) and 32 Municipios (out of 2450) in Mexico subject to our analysis.

To assess our scheme's performance quantitatively, we analyzed data in the past, when the uncertainty in the estimation of the effective reproduction number, R_t , is small, and compare it with our predictions at that date. On November 25, 2020, we observed a period starting three months before, from August 24 to September 23, and compared our nowcast prediction \hat{R}_t with R_t for each of the 32 states of Mexico (see Figure 6). Our method outputs \hat{R}_t as a distribution which spread grows as the prediction approaches the current date. For the performance assessment, we characterize the distribution of \hat{R}_t with its mean \bar{R}_t and one standard deviation at each side. To evaluate the performance, we obtain the root mean squared error, RMSE, between R_t and the prediction band created by \bar{R}_t and one standard deviation σ (see Figure 7(a)) as

$$\text{RMSE} = \sqrt{\frac{1}{n} \left(\sum_{R_t^i < \bar{R}_t - \sigma_i} (R_t^i - (\bar{R}_t^i - \sigma_i))^2 + \sum_{R_t^i > \bar{R}_t + \sigma_i} (R_t^i - (\bar{R}_t^i + \sigma_i))^2 \right)}, \quad (11)$$

where n is the number of points that meet the logical conditions. One observes that for states such as Guerrero, Jalisco, and Sinaloa, with an RMSE of 0.0, 0.001, 0.010, the band of uncertainty frequently includes the value of R_t , while for Michoacan de Ocampo, Morelos and Baja

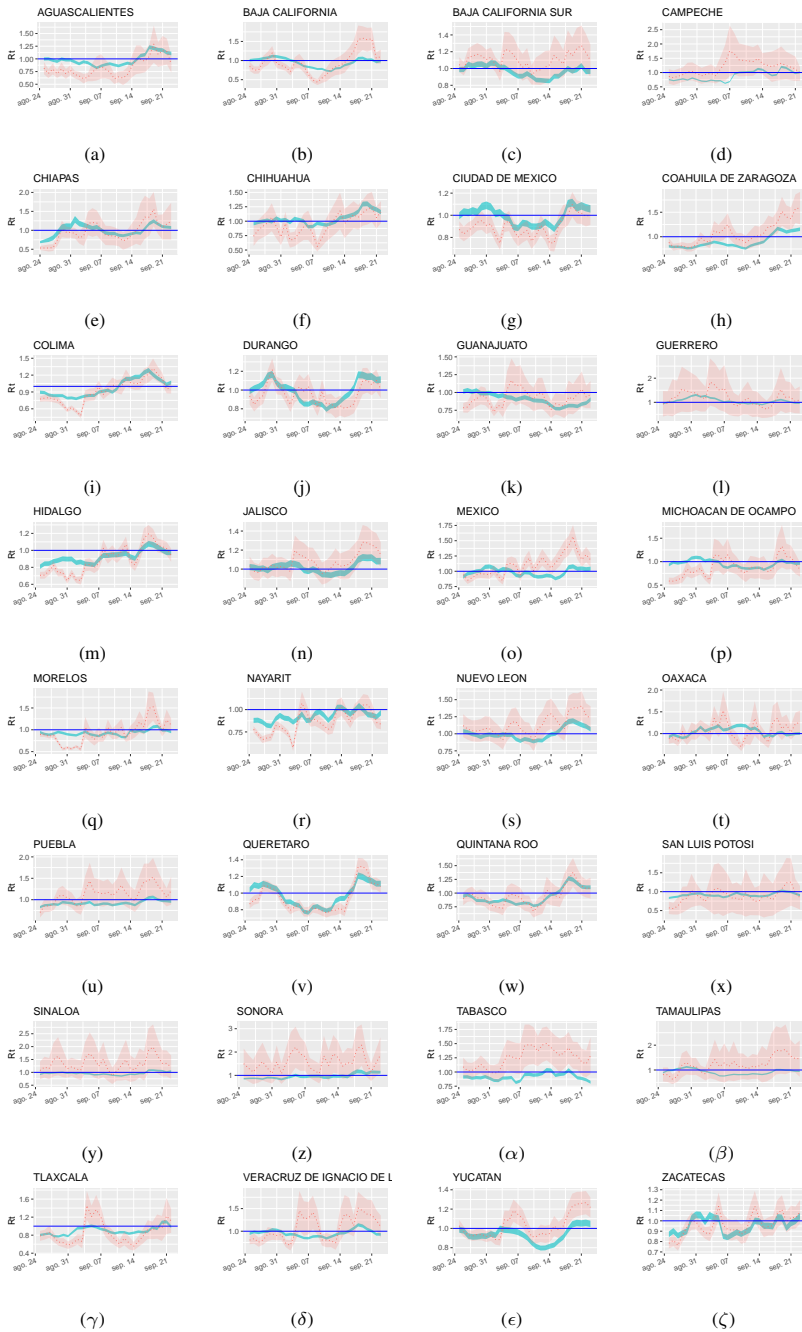
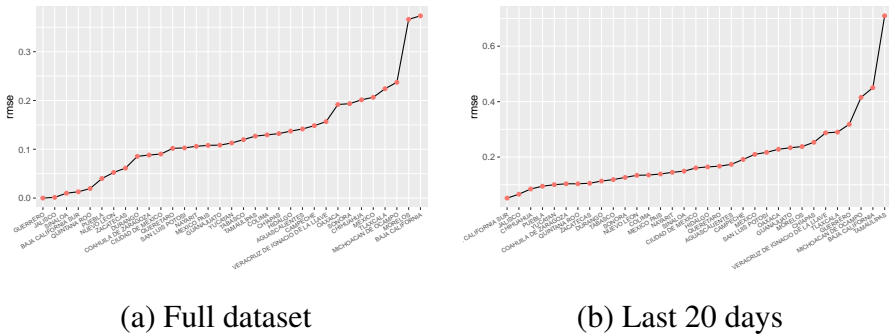


Figure 6. Effective reproduction number R_t . On November 26, 2020, we revisited the R_t (green band) that occurred and the \hat{R}_t predicted (red band) between August 24 and September 23. The green band is thick because there were still some updates, affecting registers three months before.
 Prepared using `sagej.cls`



(a) Full dataset

(b) Last 20 days

Figure 7. Nowcasting performance. We computed the RMSE for the values out of the band defined between the mean \bar{R}_t and one standard deviation σ . In (a), we use all the distributions of cases available for nowcasting. In (b), we use the most recent 20 distributions.

California, with an RMSE of 0.237, 0.366, 0.373, the value of R_t is sometimes outside the band of uncertainty.

An intriguing question is whether one should employ the whole sequence of reports to construct the frequency distributions for ρ or select the more recent ones, under the rationale that the infectious dynamics have changed or health institutions have implemented new reporting practices. To study this effect, we repeated the performance evaluation previously described but used the last 20 available distributions. In Figure 7(b), with a maximum RMSE above 0.7 and a generally more step curve, we show that the performance declines when we use the last observations compared with using the full set.

Discussion and Conclusion

Lack of testing is a significant issue in Mexico. Despite frequent suggestions by the World Health Organization, the number of tests performed normalized by its populations is low among the worst-hit countries²⁹. Thus, a data-driven approach, such as ours, is likely to underrepresent the phenomenon's true nature. Also, we need further studies to assess the effects of novel testing methods with potentially faster turnaround and the implementation of improved procedures to generate, process, analyze, and transfer information. However, our evidence suggests that our method works best, using even the information developed since the epidemic's onset.

In this document, we have presented a nowcasting method to estimate the number of confirmed positives. We have shown that this may be the foundation to generate plausible sequences out of which one may determine useful epidemic tracking indicators, such as the basic reproduction number. Our method naturally expresses uncertainty due to the lack of information but eventually gains certainty as more data accumulates.

Our method's strength is that it is based on the self-reported onset of symptoms, in contrast to other methods that use the number of confirmed positives cases accumulated by the report's day to infer this quantity. A potential drawback of our approach is that it relies on a regularity of the update cycle. As researchers implement more sophisticated systems for testing and reporting, the statistics may change. To remedy this potential effect, one may eliminate old observations and update the distributions for ρ_t regularly. Due to the difference between the incubation and latent periods, and delays in the detection and reporting cycle, our model estimates R_t up to several days in the past. We decided to take no further assumptions about the progression of the epidemic. Although potentially some form of state estimation may be possible to implement to fill the gap.

We believe that it is crucial to continue developing solutions to quickly, robustly, and reliably estimate indicators such as the basic reproduction number. A possible direction for future research may be to determine the disaggregation level to continue to generate a reliable indicator. The resulting nowcasting methods should compensate for the delays inherent in producing and processing information about this critical, global, and urgent problem. Also, we are planning to study the extend at which our model can be incorporated into dynamics-based models. This enhancement could offer improved nowcasting.

Acknowledgements

We thank Carlo Tomasi, Duke University, for providing the fundamental idea for our approach. Thanks to Dagoberto Pulido for implementing Abbott *et al.*²² to generate (c).

Author biography

Joaquín Salas is a professor in the field of Computer Vision at Instituto Politécnico Nacional. Member of the Mexican National Research System, his research interests include the monitoring

of natural systems using visual perception and aerial platforms. Salas received a Ph.D. in computer science from ITESM, México. He has been a visiting scholar at Stanford University, Duke University, Oregon State University, Xerox PARC, the Computer Vision Center, and the École Nationale Supérieure des Télécommunications de Bretagne. He has served as co-chairperson of the Mexican Conference for Pattern Recognition three times. Salas was Fulbright scholar for the US State Department. He has been invited editor for Elsevier Pattern Recognition and Pattern Recognition Letters. For his services at the Instituto Politécnico Nacional, he received the *Lázaro Cárdenas* medal from the President of Mexico.

Declaration of conflicting interests

The author declared no potential conflicts of interest with respect to the research, authorship, and/or publication of this article.

Funding

This work was partially funded by SIP-IPN 20201357.

Supplemental material

To foster further research, allowing other researchers to verify our results and serve as a stepping stone, we make our code publicly available at <https://www.github.com/joaquinsalas/nowcastingRt>.

References

1. Pueyo T. Coronavirus: The Hammer and the Dance. *Medium* 2020; 18.
2. Ma J. Estimating epidemic exponential growth rate and basic reproduction number. *Infectious Disease Modelling* 2020; 5: 129–141.
3. Secretaría de Salud, México. Datos Abiertos: Información Referente a Casos COVID-19 en México. <https://tinyurl.com/mexico-covid>, 2020. Accessed: 2020-07-11.
4. Bahl P, Doolan C, de Silva C et al. Airborne or droplet precautions for health workers treating COVID-19? *The Journal of Infectious Diseases* 2020; .
5. Nishiura H, Kobayashi T, Miyama T et al. Estimation of the asymptomatic ratio of novel coronavirus infections (COVID-19). *International Journal of Infectious Diseases* 2020; 94: 154.
6. Li R, Pei S, Chen B et al. Substantial undocumented infection facilitates the rapid dissemination of novel coronavirus (SARS-CoV-2). *Science* 2020; 368(6490): 489–493.
7. He X, Lau E, Wu P et al. Temporal dynamics in viral shedding and transmissibility of covid-19. *Nature Medicine* 2020; 26(5): 672–675.
8. Byrne A, McEvoy D, Collins A et al. Inferred duration of infectious period of SARS-CoV-2: rapid scoping review and analysis of available evidence for asymptomatic and symptomatic COVID-19 cases. *medRxiv* 2020; .

9. Garg S. Hospitalization rates and characteristics of patients hospitalized with laboratory-confirmed coronavirus disease 2019—COVID-NET, 14 States, March 1–30, 2020. *Morbidity and Mortality Weekly Report* 2020; 69.
10. Murray C. Forecasting COVID-19 impact on hospital bed-days, ICU-days, ventilator-days and deaths by US state in the next 4 months. *MedRxiv* 2020; .
11. Salas J, Pulido D, Montoya O et al. Data-Driven Inference of COVID-19 Clinical Outcome. *arXiv:submit/3270535* 2020; .
12. Wang L, Wang G, Gao L et al. Spatiotemporal dynamics, nowcasting and forecasting of COVID-19 in the United States. *arXiv:200414103* 2020; .
13. Balabdaoui F and Mohr D. Age-stratified model of the COVID-19 epidemic to analyze the impact of relaxing lockdown measures: nowcasting and forecasting for Switzerland. *medRxiv* 2020; .
14. Masjedi H, Rabajante JF, Bahrnizadd F et al. Nowcasting and Forecasting the Spread of COVID-19 in Iran. *medRxiv* 2020; .
15. Richards F. A flexible growth function for empirical use. *Journal of Experimental Botany* 1959; 10(2): 290–301.
16. Contaldi C. Covid-19: Nowcasting reproduction factors using biased case testing data. *arXiv:200512252* 2020; .
17. Annan J and Hargreaves J. Model calibration, nowcasting, and operational prediction of the COVID-19 pandemic. *medRxiv* 2020; .
18. Altmejd A, Rocklöv J and Wallin J. Nowcasting Covid-19 statistics reported withdelay: a case-study of Sweden. *arXiv:200606840* 2020; .
19. Pollock K. Modeling capture, recapture, and removal statistics for estimation of demographic parameters for fish and wildlife populations: Past, present, and future. *Journal of the American Statistical Association* 1991; 86(413): 225–238.
20. Schneble M, De Nicola G, Kauermann G et al. Nowcasting fatal COVID-19 infections on a regional level in Germany. *arXiv:200507452* 2020; .
21. Chitwood M, Russi M, Gunasekera K et al. Bayesian nowcasting with adjustment for delayed and incomplete reporting to estimate COVID-19 infections in the United States. *medRxiv* 2020; .
22. Abbott S, Hellewell J, Thompson R et al. Estimating the time-varying reproduction number of SARS-CoV-2 using national and subnational case counts. *Wellcome Open Research* 2020; 5(112): 112.
23. Menni C, Valdes A, Freidin M et al. Real-time tracking of self-reported symptoms to predict potential COVID-19. *Nature Medicine* 2020; : 1–4.
24. Petruzzi G, De Virgilio A, Pichi B et al. COVID-19: Nasal and oropharyngeal swab. *Head & Neck* 2020; 42(6): 1303–1304.
25. Long C, Xu H, Shen Q et al. Diagnosis of the Coronavirus disease (COVID-19): rRT-PCR or CT? *European Journal of Radiology* 2020; : 108961.
26. Yang W and Yan F. Patients with RT-PCR-confirmed COVID-19 and normal chest CT. *Radiology* 2020; 295(2): E3–E3.
27. Cori A, Ferguson N, Fraser C et al. A new framework and software to estimate time-varying reproduction numbers during epidemics. *American Journal of Epidemiology* 2013; 178(9): 1505–1512.

28. Bar-On Y, Flamholz A, Phillips R et al. SARS-CoV-2 (COVID-19) by the numbers. *Elife* 2020; 9: e57309.
29. Shams S, Haleem A and Javaid M. Analyzing COVID-19 pandemic for unequal distribution of tests, identified cases, deaths, and fatality rates in the top 18 countries. *Diabetes & Metabolic Syndrome: Clinical Research & Reviews* 2020; 14(5): 953–961.